Yu-Ming Chu, M. Ijaz Khan*, Hassan Waqas, Umar Farooq, Sami Ullah Khan and Mubbashar Nazeer

Numerical simulation of squeezing flow Jeffrey nanofluid confined by two parallel disks with the help of chemical reaction: effects of activation energy and microorganisms

https://doi.org/10.1515/ijcre-2020-0165
Received September 3, 2020; accepted January 20, 2021; published online February 10, 2021

Abstract: The utilization of nano-materials in a base fluid is a new dynamic technique to improve the thermal conductivity of base fluids. The suspension of tiny nanoparticles in base fluids is referred to the nano-materials. Nanofluids play a beneficial contribution in the field of nanotechnology, heat treatment enhancement, cooling facilities, biomedicine, bioengineering, radiation therapy and in military fields. The analysis of bioconvection characteristics for unsteady squeezing flow of non-Newtonian Jeffery nanofluid with swimming microorganisms over parallel disks with thermal radiation and activation energy has been studied in this continuation. The motivations for performing current analysis are to inspect the heat transfer enhancement in Jeffrey nanofluid in presence of multiple thermal features. The Jeffrey nanofluid contains motile microorganisms which convey dynamic applications in bio-technology and medical sciences and agricultural engineering. The system comprising differential equations of derivative is restricted to an ordinary one by means of a sufficient dimensionless similarity vector, and then implemented numerically by means of a famous shooting scheme with MATLAB tools. The effect of the significant parameters over the fluid flow is investigated from a physical point of view. The numerical findings of the modeled system are explored in detail using tabular data.

Keywords: Jeffery nanofluid; numerical scheme; thermal radiation; squeezing bioconvection flow.

***Corresponding author: M. Ijaz Khan,** Department of Mathematics and Statistics, Riphah International University, I-14, Islamabad 44000, Pakistan, E-mail: mikhan@math.qau.edu.pk
Yu-Ming Chu, Department of Mathematics, Huzhou University, Huzhou 313000, P. R. China; and Hunan Provincial Key Laboratory of Mathematical Modeling and Analysis in Engineering, Changsha University of Science & Technology, Changsha 410114, P. R. China
Hassan Waqas and Umar Farooq, Department of Mathematics, Government College University Faisalabad, Layyah Campus, Layyah 31200, Pakistan
Sami Ullah Khan, Department of Mathematics, COMSATS University Islamabad, Sahiwal 57000, Pakistan
Mubbashar Nazeer, Department of Mathematics, Institute of Arts and Science, Government College University Faisalabad, Chiniot Campus, Chiniot, Pakistan

1 Introduction

1.1 Overview

The synthesis of nanofluids has drawn valuable attention of many scientists and engineers due to their significances in various areas of thermal engineering and industrial applications. Owing to the wide range of applications of nanofluid in various technological and industrial processes like cooling of electronic components, sanitization of pharmaceutical suspensions, thermal steam generation and aerospace molecular biology, many contributions are performed on this topic specially in current century. In nano-materials, nano-sized particles (1–100 nm) are discharged into base liquids (water, car gasoline, methanol, ethylene and glycerin) to improve the heat conductivity of base fluids. In addition, a wide variety of businesses is practically aware of applications for nano-liquids. The use of nanofluids involves heat exchangers, generators, light and heavy equipment, alternative energy sources, thermal efficiency systems, nuclear reactors, electrical cooling components, combustion, medicines, etc. Choi (1995) proposed the idea of developing the thermal performance of natural liquids by nanoparticles. Nanotechnology has also resolved a host of issues related to the flow of heat in factories. They can be classified as heat transfer nanofluids, bio-and medicinal nanofluids, extraction and environmental nanofluids, etc. Buongiorno (2006) suggested a critical character in the creation of a non-homogenous technological combination for the convective manufacturing of nano-materials with heat transfer constraints. Ramzan et al. (2020a) found the nanofluid flow with autocatalytic chemical reactions about such a vertical sheet with thermal radiation and slipping conditions. Katta and Jayavel (2020) are researching the increase in heat transfer in the radiative peristaltic motion of nanofluid over a stretching of a compelling magnetic field. Turkyilmazoglu (2020) explores the impact of single-phase nanofluid on material and fluid spectacle and tests its linear stability. Modified concept of homogeneous-heterogeneous reactions in flow of Casson material is inspected by Khan et al. (2017). Li et al. (2020) exemplified the numerical investigation of the effect of nanofluid during the melting process. Research on MHD flows of Newtonian or non-Newtonian nanofluids across stretching sheets has inspired a variety of researchers based on their various uses in different sectors and environmental applications including such polymer extrusion, material synthesis, paper manufacturing, condensation, polystyrene manufacturing, and glass blowing and so on. Atif, Hussain, and Sagheer (2019) considered the motion of heterogeneous bio-convective fluids with nano-materials and gyrostatic microorganisms. Hosseinzadeh et al. (2020) investigate the MHD flow of microorganisms and nano-materials on the soil. Aleem et al. (2020) investigate the unsteady, radiative, continuous flow of Jeffrey fluid through a porous medium of a magnetic field between two perpendicular plastic surfaces fixed in a fluid flow. Babu, Venkateswarlu, and Keshava Reddy (2019) explore the slow, radiative, constant flow of Jeffrey fluid under the influence of a magnetic field between two diagonal plates fixed in a fluid medium. Sajjad et al. (2020) analyze the current study to provide an (MHD) study of Jeffrey nanofluid flow caused by a curved stretchable surface. The rheological system appears for the use of nonlinear thermal radiation. Some of the articles by different investigator in present years can be perceived through the references (Anwar, Kumam, and Watthayu 2020; Bozorg et al. 2020; Ghasemi and Siavashi 2020; Imran et al. 2020; Khan et al. 2020; Rasool, Shafiq, and Tlili 2020; Saffarian, Moravej, and Doranehgard 2020; Yang, Du, and Zhang 2020).

Bioconvection was of course, observed on average because of the upward migration of microorganisms. Bioconvection phenomenon includes applications for bio-microsystems including such biomaterials and biotechnology. In comparison, the bioconvection approach concerns a targeted swimming cell linked to the species of motile microorganisms. The physiological value of bioconvection has been successfully established in bio-fuels, ethanol and numerous manufacturing and environmental technologies. The incorporation of motile microorganisms into solutions has numerous uses, including such bio-micro technologies (bioengineering and enzyme biosensors), micro-fluidics for improving volatility in nano-liquids and for enhancing the mass transport method. A precise theoretical consequence of bioconvection in nanofluids has recently been developed. The wonder of bioconvection seems to have taken place in separate eras of biology and biotechnology. Kuznetsov (2011) studied nanofluid bioconvection in the presence of microorganisms and nano-materials. Waqas et al. (2019a) explore the phenomena of Williamson nanofluid in the occurrence of a motile microorganism for a time-dependent magnetohydrodynamic flow. Khan et al. (2019) thermal radiation research and motile species Oldroyd-B nanofluid flow study. Alshomrani and Ramzan (2019) explored the consequence of the ferromagnetic dipole on the nanofluid flow via the stretched cylinder. Alwatban et al. (2019) was studying the bioconvection of magnetized nanoparticles. Tlili et al. (2019) explored the characteristics of second-order bioconvection slips on Oldroyd-B nano-liquids. Waqas et al. (2019b) regulates the computational function of the electromagnetic aspect of the viscous nanofluid through disk in the occurrence of microorganisms. Ramzan et al. (2020b) examined nanofluid flow through Hall and Ion sliding together with activation energy, microorganisms, and Cattaneo–Christov heat and flux.

Current continuation explores the bioconvection analysis for radiative flow of Jeffrey nanofluid with swimming of microorganisms induced by two parallel disks. The activation energy features are also incorporated. The modeled flow problem is numerically solved with help of shooting algorithm. A comprehensive graphical illustration is carried out for inspecting insight physical consequences. Some other important research on such topic can

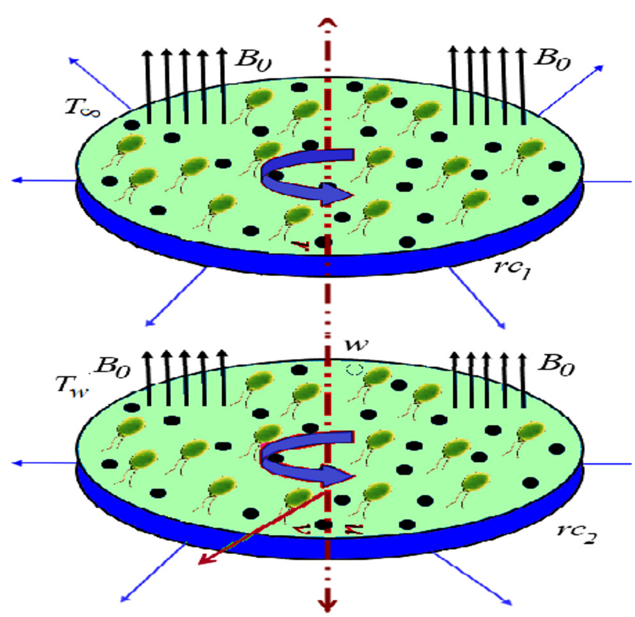

Figure 1: Flow problem representation.

be listed in Refs. Khan and Alzahrani (2021a, 2021b), Khan et al. (2021) and Nazeer et al. (2021).

2 Mathematical description of problem

Let us assume a two-dimensional unsteady squeezing flow of Jeffery nanofluid with gyrotactic motile microorganisms between two parallel disks (Figure 1). The activation energy and thermal radiation impacts are also considered. The ambient temperature, concentration T_∞, C_∞ and microorganisms are N_∞. The induce magnetic field and external electric field are neglected owing to small Reynolds number.

The main assumptions for present phenomenon are listed below:

- Unsteady two-dimensional squeezing flow has been considered.
- Jeffery fluid model is adopted to examine the rheological consequences.
- Effect of thermal radiation and activation energy are utilized.
- The magnetic force impact is considered by taking it in perpendicular direction.

The governing equations for radiative flow Jeffrey nanofluid with motile microorganism are (Khan et al. 2020; Turkyilmazoglu 2020):

$$\frac{\partial u}{\partial r}+\frac{u}{r}+\frac{\partial w}{\partial z}=0, \tag{1}$$

$$\begin{aligned}
&\frac{\partial u}{\partial t}+u\frac{\partial u}{\partial r}+w\frac{\partial w}{\partial z}=-\frac{1}{\rho}\frac{\partial p}{\partial r}+\frac{\nu}{1+\lambda_1}\left(\frac{\partial^2 u}{\partial r^2}+\frac{\partial^2 u}{\partial z^2}+\frac{1}{r}\frac{\partial u}{\partial r}-\frac{u}{r^2}\right)\\
&+\frac{\nu\lambda_2}{1+\lambda_1}\left(\begin{array}{l}
\frac{\partial^3 u}{\partial t\,\partial z^2}+2\frac{\partial^3 u}{\partial t\,\partial r^2}+\frac{2}{r}\frac{\partial^2 u}{\partial t\,\partial z}+\frac{\partial^3 w}{\partial t\,\partial r\,\partial z}-\frac{2}{r^2}\frac{\partial y}{\partial t}+\frac{\partial u}{\partial t}\left(\frac{\partial^2 u}{\partial r^2}-2\frac{u}{r^2}\right)+\frac{\partial w}{\partial r}\frac{\partial^2 w}{\partial r\,\partial z}\\
+u\left(\frac{\partial^3 u}{\partial r^3}+\frac{\partial^3 w}{\partial r^2\,\partial z}+\frac{\partial^3 u}{\partial r\,\partial z^2}+2\frac{u}{r^3}\right)+w\left(\frac{\partial^3 u}{\partial z\,\partial r^2}+\frac{2}{r}\frac{\partial^2 u}{\partial r\,\partial z}+\frac{\partial^3 w}{\partial z^3}+\frac{\partial^2 w}{\partial r\,\partial z}\right)\\
+\frac{\partial u}{\partial z}\left(\frac{\partial^2 w}{\partial r^2}-2\frac{w}{r^2}+\frac{\partial^2 u}{\partial z\,\partial r}\right)+\frac{\partial w}{\partial z}\left(\frac{\partial^2 u}{\partial r^2}+\frac{\partial^2 w}{\partial r\,\partial z}\right)+\frac{2}{r}\frac{\partial^2 u}{\partial r^2}
\end{array}\right)\\
&-\frac{\sigma B^2}{\rho_f}u+\frac{1}{\rho_f}\left[\begin{array}{l}(1-C_f)\rho_f\beta^* g^*(T-T_\infty)-(\rho_p-\rho_f)g^*(C-C_\infty)\\ -(N-N_\infty)g\gamma^{**}(\rho_m-\rho_f)\end{array}\right],
\end{aligned} \tag{2}$$

$$\begin{aligned}
&\frac{\partial u}{\partial t}+u\frac{\partial u}{\partial r}+w\frac{\partial w}{\partial z}=-\frac{1}{\rho}\frac{\partial p}{\partial z}+\frac{\nu}{1+\lambda_1}\left(\frac{\partial^2 w}{\partial r^2}+\frac{\partial^2 w}{\partial z^2}+\frac{1}{r}\frac{\partial w}{\partial r}\right)\\
&+\frac{\nu\lambda_2}{1+\lambda_1}\left(\begin{array}{l}
\frac{\partial^3 w}{\partial t\,\partial r\,\partial z}+\frac{\partial^3 u}{\partial t\,\partial r^2}+2\frac{\partial^3 u}{\partial r\,\partial z^2}+2\frac{\partial u}{\partial z}\frac{\partial^2 w}{\partial r\,\partial z}+\frac{\partial u}{\partial r}\left(\frac{\partial^2 u}{\partial r\,\partial z}+\frac{\partial^2 w}{\partial r^2}\right)\\
+u\left(\frac{\partial^3 w}{\partial r^2\,\partial z}+\frac{\partial^3 u}{\partial r^3}\right)+\frac{\partial w}{\partial r}\left(\frac{\partial^2 u}{\partial z^2}+\frac{\partial^3 u}{\partial t\,\partial z^2}\right)+w\left(\begin{array}{l}\frac{\partial^3 u}{\partial r\,\partial z^2}+\frac{\partial^3 w}{\partial r^2\,\partial z}+\frac{\partial^3 w}{\partial z^3}\\ +\frac{1}{r}\frac{\partial^2 u}{\partial z^2}+\frac{1}{r}\frac{\partial^2 w}{\partial z\,\partial r}\end{array}\right)\\
+\frac{u}{r}\left(\frac{\partial^2 u}{\partial r\,\partial z}+\frac{\partial^2 w}{\partial r^2}\right)+\frac{1}{r}\left(\frac{\partial^2 u}{\partial t\,\partial z}+\frac{\partial^2 w}{\partial t\,\partial r}\right)
\end{array}\right),
\end{aligned} \tag{3}$$

$$\begin{aligned}
&\frac{\partial T}{\partial t}+u\frac{\partial T}{\partial r}+w\frac{\partial T}{\partial z}=\alpha\left(\frac{\partial^2 T}{\partial r^2}+\frac{1}{r}\frac{\partial T}{\partial r}+\frac{\partial^2 T}{\partial z^2}\right)+\tau\left(\begin{array}{l}D_B\left(\frac{\partial C}{\partial r}\frac{\partial T}{\partial r}+\frac{\partial C}{\partial z}\frac{\partial T}{\partial z}\right)+\frac{D_T}{T_m}\left(\frac{\partial T}{\partial r}\right)^2\\ +\left(\frac{\partial T}{\partial z}\right)^2\end{array}\right)\\
&+\frac{16\gamma^{**}T_\infty^3}{3\rho c_p k^*}\left(\frac{\partial^2 T}{\partial y^2}\right),
\end{aligned} \tag{4}$$

$$\frac{\partial C}{\partial t}+u\frac{\partial C}{\partial r}+w\frac{\partial C}{\partial z}=D_B\left(\frac{\partial^2 C}{\partial r^2}+\frac{1}{r}\frac{\partial TC}{\partial r}+\frac{\partial^2 C}{\partial z^2}\right)$$
$$+\frac{D_T}{T_m}\left(\frac{\partial^2 T}{\partial r^2}+\frac{1}{r}\frac{\partial TT}{\partial r}+\frac{\partial^2 T}{\partial z^2}\right)$$
$$-Kr^2(C-C_\infty)\left(\frac{T}{T_\infty}\right)^n\exp\left(\frac{-E_a}{kT}\right), \quad (5)$$

$$\frac{\partial N}{\partial t}+u\frac{\partial N}{\partial r}+w\frac{\partial N}{\partial z}+\frac{bW_c}{(C_w-C_\infty)}\left[\frac{\partial}{\partial z}\left(N\frac{\partial C}{\partial z}\right)\right]$$
$$=D_m\left(\frac{\partial^2 N}{\partial z^2}\right), \quad (6)$$

with boundary conditions

$$\left.\begin{array}{l} u=0, w=-w_0, T=T_w, C=C_w, N=N_w \text{ at } z=0,\\ u=0, w=\frac{\partial h}{\partial t}, T=T_h, C=C_h, N=N_h \text{ at } z=h(t). \end{array}\right\} \quad (7)$$

Here, the velocity components are denoted by (u, w) along the (r, z) directions, respectively, (p) is pressure, (μ) stand for the dynamic viscosity, (ρ) shows the density of base fluid, (C) the concentration, (σ) is denotes the electrical conductivity, $\tau(=(\rho c)_p/(\rho c)_f)$ depicts the ratio of heat capacity and heat capacity of fluid, (D_B)denotes the Brownian diffusion coefficient, $\alpha(=k/(\rho c)_f)$ stand for the thermal diffusivity, (T_m) the mean fluid temperature, (λ_1) signify the ratio of relaxation and retardation times, (λ_2) is the retardation time, respectively, $(T)$is the temperature, the kinematic viscosity $\nu(=\mu/\rho)$, $(\rho c)_p$ stand for the effective heat capacity of nanoparticles, $(\rho c)_f$ is the heat capacity of fluid, (D_T) is the thermophoresis diffusion coefficient and (k) the thermal conductivity. Let us introduce following dimensionless quantities:

$$\left.\begin{array}{l} u=\alpha r/2(1-\alpha t)f'(\zeta), w=-\alpha H\big/\sqrt{(1-\alpha t)}f\\ (\zeta), \zeta=z\big/H\sqrt{(1-\alpha t)}, \theta(\zeta)=T-T_h/T_w-T_h, \phi(\zeta)\\ =C-C_h/C_w-C_h, \chi(\zeta)=N-N_h/N_w-N_h \end{array}\right\}, \quad (8)$$

Equation (1) is automatically satisfied, after introducing Eq. (8) in Eqs. (2)–(6) reduce to following non-dimensional system

$$f^{iv}-Sq(1+\lambda_1)(\zeta f'''+3f''-2ff''')+\frac{\beta}{2}(\zeta f^{v}+5f^{iv}+f'f'''-3f'f^{iv})$$
$$-M^2(1+\lambda_1)f''+\mathrm{Re}\lambda(\theta-\mathrm{Nr}\phi-\mathrm{Nc}\chi)=0, \quad (9)$$

$$\left(1+\frac{4}{3}Rd\right)\theta''+\mathrm{PrSq}(f\theta'-\zeta\theta')+\mathrm{PrNb}\theta'\phi'+\mathrm{Pr}Nt\theta'^2=0, \quad (10)$$

$$\phi''+\mathrm{PrLeSq}(f\phi'-\zeta\phi')+\frac{Nt}{Nb}\theta''-\mathrm{PrLe}\sigma^*$$
$$(1+\delta\theta)^n\exp\left(\frac{-E}{(1+\delta\theta)}\right)\phi=0, \quad (11)$$

$$\chi''+\mathrm{LbSq}(f\chi'-\zeta\chi')-\mathrm{Pe}(\phi''(\chi+\delta_1)+\chi'\phi')=0 \quad (12)$$

with boundary constraints

$$\left.\begin{array}{l} f(0)=S, f'(0)=0, \theta(0)=1, \phi(0)=1, \chi(0)=1,\\ f(1)=\frac{1}{2}, f'(1)=0, \theta(1)=0, \phi(1)=0, \chi(1)=0. \end{array}\right\}, \quad (13)$$

where $\mathrm{Pr}(=\nu/\alpha)$ be Prandtl number, $\mathrm{Nb}(=\tau D_B(C_w-C_h)/\nu)$ Brownian motion parameter, $\mathrm{Nt}(=\tau D_T(T_w-T_h)/T_m\nu)$ the thermophoresis parameter, $M\left(=HB_0\sqrt{\frac{\sigma}{\mu}}\right)$ the Hartman number and $S(=w_0/\alpha H)$ the suction/blowing parameter, $\mathrm{Le}(=\alpha/D_B)$ the Lewis number, radiation parameter $\mathrm{Rd}(=4\gamma^*T_\infty^3/kk^*)$, $\mathrm{Nr}=((\rho_p-\rho_f)(C_w-C_\infty)/\rho_f(1-C_\infty)(T_w-T_\infty)\beta^{**})$, buoyancy ratio parameter, $\mathrm{Nc}=(\gamma(\rho_m-\rho_f)(N_w-N_\infty)/\rho_f(1-C_\infty)(T_w-T_\infty)\beta^{**})$, bioconvection Rayl eigh number mixed convection parameter $\lambda=(\beta^{**}g(1-C_\infty)(T_w-T_\infty)r/(1-\alpha t))$, $\beta(=\lambda_2\alpha/1-\alpha t)$ the Deborah number, chemical reaction parameter and activation energy parameter are $\sigma^*=(Kr^2/\alpha)$, and $E(=E_a/kT_\infty)$, $\delta(=T_w-T_\infty/T_\infty)$ the temperature difference parameter, bioconvection Lewis number is $\mathrm{Lb}(=\nu/D_m)$, $\mathrm{Pe}(=bW_c/D_m)$ the Peclet number $\mathrm{Sq}(=\alpha H^2/2\nu)$ the squeezing parameter.

Expressions of the tension of the skin relating to the lower and upper disk

$$Cf_1=\frac{\tau_{rz}|_{z=0}}{\rho\left(\frac{\alpha H}{2(1-\alpha t)^{\frac{1}{2}}}\right)^2}, \quad (14)$$

$$Cf_2=\frac{\tau_{rz}|_{z=h(t)}}{\rho\left(\frac{\alpha H}{2(1-\alpha t)^{\frac{1}{2}}}\right)^2}, \quad (15)$$

with

$$\tau_{rz}=\frac{\mu}{1+\lambda_1}\left(\frac{\partial u}{\partial z}+\frac{\partial w}{\partial r}\right)+\frac{\lambda_2}{1+\lambda_1}\left(\frac{\partial^2 u}{\partial t\,\partial z}+\frac{\partial^2 w}{\partial t\,\partial r}+u\right.$$
$$\left.\left(\frac{\partial^2 u}{\partial r\,\partial z}+\frac{\partial^2 w}{\partial r^2}\right)+w\left(\frac{\partial^2 u}{\partial z^2}+\frac{\partial^2 w}{\partial z\,\partial r}\right)\right). \quad (16)$$

The dimensionless are

$$\left.\begin{array}{l} \frac{H^2}{r^2}\mathrm{Re}_r Cf_1=\left(1+\frac{3}{2}\beta\right)f''(0),\\ \frac{H^2}{r^2}\mathrm{Re}_r Cf_2=\left(1+\frac{3}{2}\beta\right)f''(1), \end{array}\right\}, \quad (17)$$

where

$$\mathrm{Re}_r^{-1} = \frac{2\nu}{r\alpha H(1+\lambda_1)(1+\alpha t)^{\frac{1}{2}}}. \quad (18)$$

$$\left.\begin{aligned} \mathrm{Nu}_{r1} &= -\frac{H}{(T_w - T_h)}\left.\frac{\partial T}{\partial z}\right|_{z=0} = -\frac{1}{\sqrt{1-\alpha t}}\theta'(0), \\ \mathrm{Nu}_{r2} &= -\frac{H}{(T_w - T_h)}\left.\frac{\partial T}{\partial z}\right|_{z=h(t)} = -\frac{1}{\sqrt{1-\alpha t}}\theta'(1), \end{aligned}\right\}, \quad (19)$$

$$\left.\begin{aligned} \mathrm{Sh}_{r1} &= -\frac{H}{(C_w - C_h)}\left.\frac{\partial C}{\partial z}\right|_{z=0} = -\frac{1}{\sqrt{1-\alpha t}}\phi'(0), \\ \mathrm{Sh}_{r2} &= -\frac{H}{(C_w - C_h)}\left.\frac{\partial C}{\partial z}\right|_{z=h(t)} = -\frac{1}{\sqrt{1-\alpha t}}\phi'(1), \end{aligned}\right\}, \quad (20)$$

3 Solution technique

The numerical process of the apparent MATLAB shooting scheme for various physiological parameters presents the structure of the intricate system of Ordinary differential equations (9)–(12) above the corresponding original and boundary state equations (13).This technique is very successful in a small step-size condition with a negligible error. The inherent scheme technique for the final expresses is defined below. By implementation of this method firstly, higher-order differential equations are changed into first-order ODEs with introducing new variables such as:

Let

$$\left.\begin{aligned} & f = g_1, f' = g_2, f'' = g_3, f''' = g_4, f^{iv} = g_5, f^{v} = g_5' \\ & \theta = g_6, \theta' = g_7, \theta'' = g_7', \phi = g_8, \phi' = g_9, \phi'' = g_9' \\ & \chi = g_{10}, \chi' = g_{11}, \chi'' = g_{11}' \end{aligned}\right\}, \quad (21)$$

$$g_5' = \frac{\begin{aligned} & -g_5 - Sq(1+\lambda_1)(\zeta g_4 + 3g_3 - 2g_1 g_4) + M^2(1+\lambda_1) g_3 \\ & + \mathrm{Re}\lambda(g_6 - \mathrm{Nr} g_8 - \mathrm{Nc} g_{10}) - \frac{\beta}{2}(5g_5 + g_3 g_4 - 3g_1 g_5) \end{aligned}}{\zeta\frac{\beta}{2}}, \quad (22)$$

$$g_7' = \frac{-\mathrm{PrSq}(g_1 g_7 - \zeta g_7) - \mathrm{PrNb} g_7 g_9 - \mathrm{PrNt} g_7^2}{\left(1 + \frac{4}{3}\mathrm{Rd}\right)}, \quad (23)$$

$$\begin{aligned} g_9' = & -\mathrm{PrLeSq}(g_1 g_9 - \zeta g_9) - \frac{\mathrm{Nt}}{\mathrm{Nb}} g_7' \\ & + \mathrm{PrLe}\sigma^*(1+\delta g_6)^n \exp\left(\frac{-E}{(1+\delta g_6)}\right) g_8, \end{aligned} \quad (24)$$

$$\begin{aligned} g_{11}' = & -LbSq(g_{10} g_{11} - \zeta g_{10}) + Pe(\underset{9}{g'}(g_{10} + \delta_1) \\ & + g_{11} g_9), \end{aligned} \quad (25)$$

with boundary constraints

$$\left.\begin{aligned} & g_1(0) = S, g_2(0) = 0, g_6(0) = 1, g_8(0) = 1, g_{10}(0) = 1, \\ & g_1(1) = \frac{1}{2}, g_2(1) = 0, g_6(1) = 0, g_8(1) = 0, g_{10}(1) = 0. \end{aligned}\right\}, \quad (26)$$

4 Graphical analysis

In this division, the major aim is to visualization the characteristics of velocity profile, temperature distribution profile, concentration distribution profile, and motile microorganisms profile against involved prominent parameters such as Deborah number, squeezing parameter, activation energy, magnetic parameter, bioconvection Rayleigh number, buoyancy ratio parameter, Prandtl number, Brownian motion parameter, thermal radiation, mixed convection parameter, thermophoresis parameter and Lewis number. In addition, bioconvection Lewis number and Peclet number are also discussed. Figure 2 survey the outcome mixed convection parameter λ and squeezing parameter Sq on velocity profile f'. The flow of fluid upsurges in scenario of enhanced mixed convection parameter λ magnitudes. Additional from these curves lines it can be captured that velocity profile f' also boom for larger squeezing parameter Sq. Figure 3 is noticed to show the inspiration of magnetic parameter M and Nr versus velocity profile f'. It is investigated velocity profile f' reduced by growing the variations of magnetic parameter M and buoyancy ratio parameter Nr. Practically, a greater magnetic parameter creates Lorenz forces that minimize fluid flow. Features of Deborah number β and Nc via velocity profile f' is sketched in Figure 4. Here velocity profile f' diminished by booming the variation of Deborah number β and Nc. Figure 5 provides the information about the impact of Prandtl number Pr and Deborah number for thermal radiation Rd on temperature distribution profile θ. Clearly temperature distribution profile θ decline for higher estimation Prandtl number Pr, because it show opposite performance for thermal radiation Rd. Physically, augmented radiation variations convey additional heat to the fluid, which debates and enhancing aspect on the surface of the thermal boundary condition and the temperature of the fluid. Performance of temperature distribution profile θ under variation of Brownian motion parameter Nb and Nt is reflected in Figure 6. Here temperature distribution profile θ is a growing function of both the parameters, Nb and thermophoresis parameter Nt. Physically thermophoresis mechanisms i.e. the particles of fluid transport from hot region to cool region.

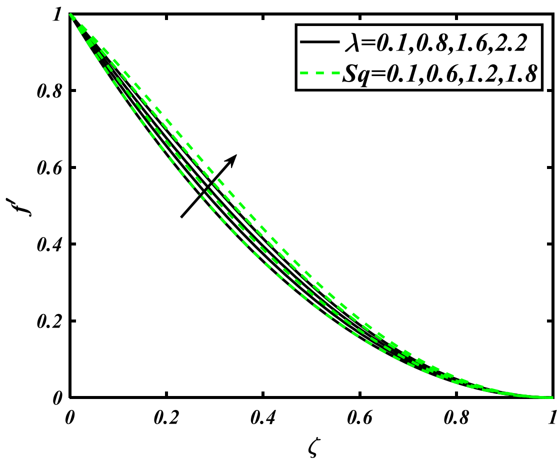

Figure 2: Change in f' for λ & Sq.

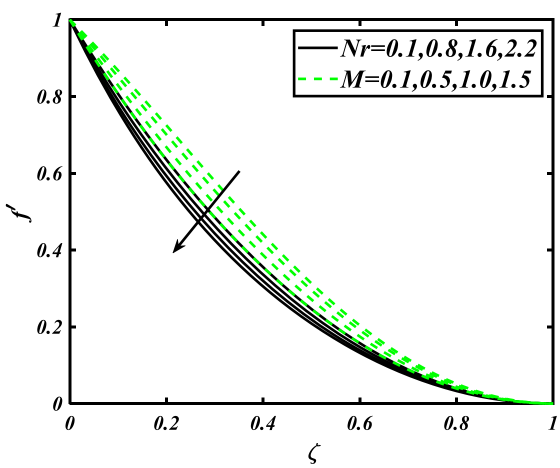

Figure 3: Change in f' for Nr & M.

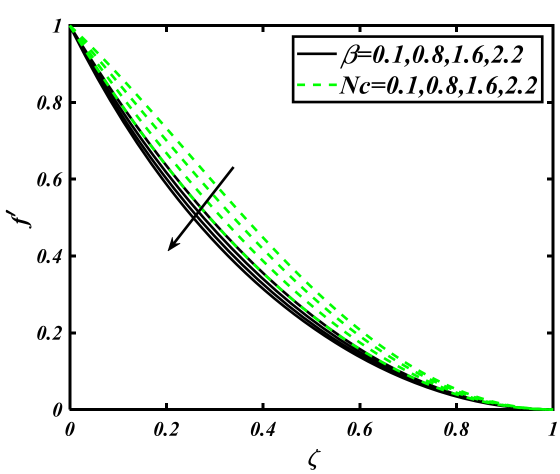

Figure 4: Change in f' for β & Nc.

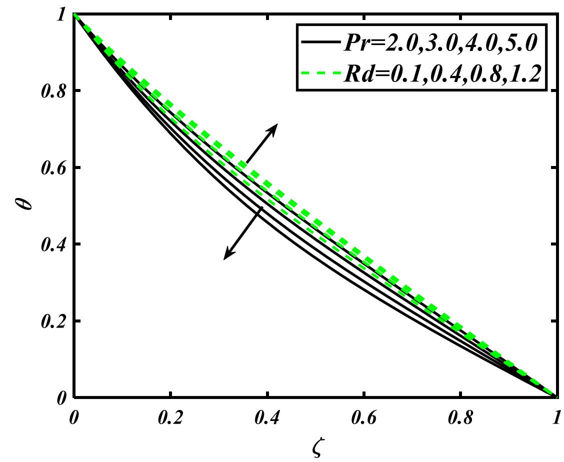

Figure 5: Change in θ for Nb & Nt.

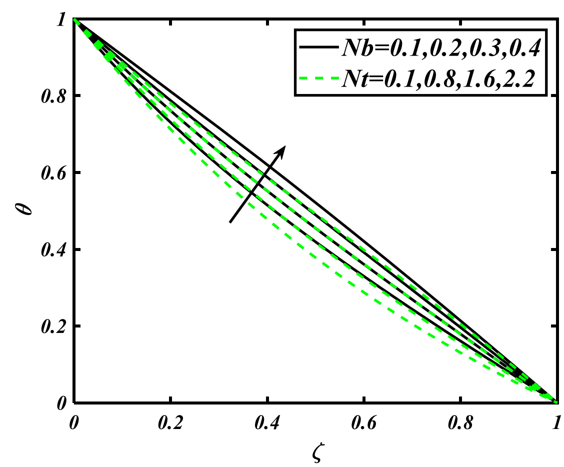

Figure 6: Change in θ for dPr & Rda.

The impact of Nt and activation energy E via concentration of nanoparticles field ϕ is displayed in Figure 7. It is noticeable that the concentration of nanoparticles profile ϕ is a diminishing role of thermophoresis parameter Nt and activation energy E. Figure 8 displays the characteristics of concentration of nanoparticles profile ϕ versus solutal stratification Lewis number Le and Nb. It is summarized that concentration of nanoparticles profile ϕ are boomed up for advanced variations of Lewis number Le and Brownian motion parameter Nb. The impact of Pe and bioconvection Lewis number Lb on microorganism profile χ is showed through Figure 9. Here microorganism profile χ decline for larger Peclet number Pe and Lb. From Table 1 reveals that local skin friction boosted up for various estimation of M, Nr while reduced for Sq. From Tables 2 and 3 investigated that the local Nusselt number and the local Sherwood number rises for distinguished estimation of Sq and Pr. Table 4 depicts microorganism density number improved with higher Pe and Lb.

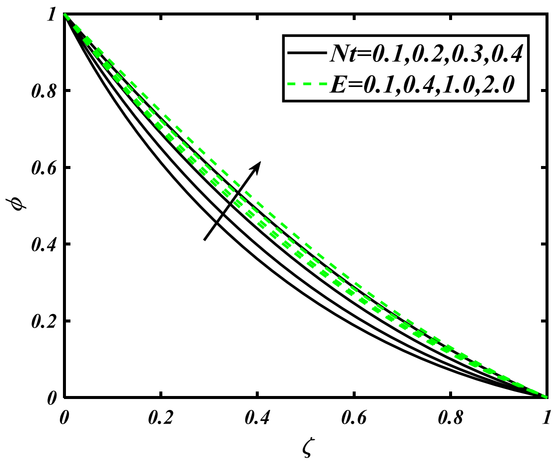

Figure 7: Change in ϕ for Nt & E.

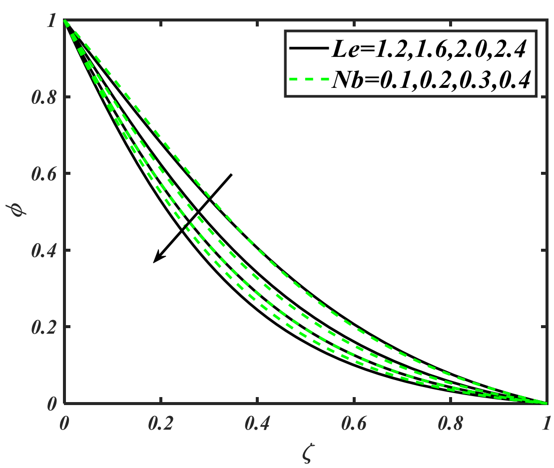

Figure 8: Change in ϕ fort Le & Nb.

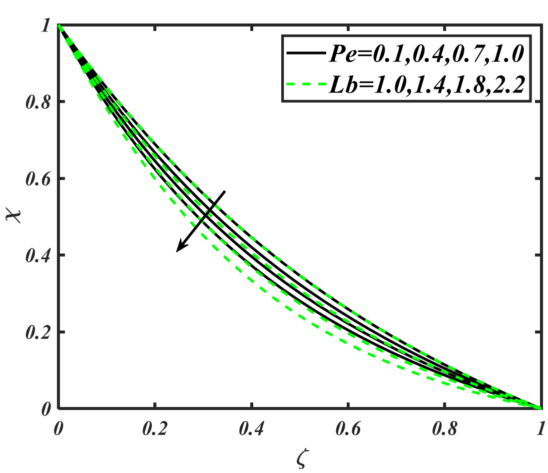

Figure 9: Change in χ for Pe & Lb.

Table 1: Numerical outcomes of $-f''(0)$ versus physical parameters.

Flow parameters					Local skin friction coefficients
M	λ	Nr	Nc	Sq	$-f''(0)$
0.3	0.1	0.5	0.5	0.1	2.0566
0.6					2.0650
0.9					2.0733
0.2	0.2	0.5	0.5	0.1	2.0528
	0.4				2.0510
	0.6				2.0491
0.2	0.1	0.1	0.5	0.1	2.0518
		0.3			2.0528
		0.7			2.0548
0.2	0.1	0.5	0.1	0.1	2.0516
			0.3		2.0527
			0.7		2.0548
0.2	0.1	0.5	0.5	0.2	2.0274
				0.4	2.0138
				0.6	2.0093

Table 2: Numerical outcomes of $-\theta'(0)$ versus physical parameters.

Flow parameters							Local Nusselt number
M	λ	Rd	Pr	Sq	Nb	Nt	$-\theta'(0)$
0.3	0.1	0.4	2.0	0.1	0.2	0.3	1.4672
0.6							1.4868
0.9							1.5064
0.2	0.2	0.4	2.0	0.1	0.2	0.3	1.4606
	0.4						1.4604
	0.6						1.4602
0.2	0.1	0.6	2.0	0.1	0.2	0.3	1.4090
		1.2					1.3075
		1.8					1.2460
0.2	0.1	0.4	3.0	0.1	0.2	0.3	1.6116
			4.0				1.7163
			5.0				1.7821
0.2	0.1	0.4	2.0	0.2	0.2	0.3	1.4914
				0.4			1.5561
				0.6			1.6216
0.2	0.1	0.4	2.0	0.1	0.1	0.3	1.5515
					0.4		1.2954
					0.8		1.0233
0.2	0.1	0.4	2.0	0.1	0.2	0.1	1.5998
						0.4	1.3964
						0.8	1.1705

Table 3: Numerical outcomes of $\phi'(0)$ versus physical parameters.

Flow parameters									Local Sherwood number
M	***λ***	**Le**	**Pr**	**Sq**	**Nb**	**Nt**	**Pe**	***E***	$\phi'(0)$
0.3	0.1	2.0	2.0	0.1	0.2	0.3	0.1	0.5	1.4446
0.6									1.4166
0.9									1.3888
0.2	0.2	2.0	2.0	0.1	0.2	0.3	0.1	0.5	1.4542
	0.4								1.4548
	0.6								1.4554
0.2	0.1	3.0	2.0	0.1	0.2	0.3	0.1	0.5	1.9831
		4.0							2.4647
		5.0							2.9058
0.2	0.1	2.0	3.0	0.1	0.2	0.3	0.1	0.5	1.7615
			4.0						2.1042
			5.0						2.4706
0.2	0.1	2.0	2.0	0.2	0.2	0.3	0.1	0.5	1.4158
				0.4					1.3297
				0.6					1.2403
0.2	0.1	2.0	2.0	0.1	0.1	0.3	0.1	0.5	0.5776
					0.4				1.8809
					0.8				2.0745
0.2	0.1	2.0	2.0	0.1	0.2	0.1	0.1	0.5	1.8088
						0.4			1.3623
						0.8			1.4747
0.2	0.1	2.0	2.0	0.1	0.2	0.3	0.2	0.5	1.6129
							0.3		1.8298
							0.4		2.0550
0.2	0.1	2.0	2.0	0.1	0.2	0.3	0.1	0.2	1.3414
								0.4	1.3298
								0.6	1.3188

Table 4: Numerical outcomes solutions of $-\chi'(0)$ versus physical parameters.

Flow parameters					Local microorganism number
M	***λ***	**Sq**	**Lb**	**Pe**	$-\chi'(0)$
0.3	0.1	0.1	2.0	0.1	1.4026
0.6					1.3966
0.9					1.3907
0.2	0.2	0.1	2.0	0.1	1.4047
	0.4				1.4049
	0.6				1.4051
0.2	0.1	0.2	2.0	0.1	1.3977
		0.4			1.3807
		0.6			1.3630
0.2	0.1	0.1	3.0	0.1	1.6202
			4.0		1.8820
			5.0		2.0681
0.2	0.1	0.1	2.0	0.2	1.6229
				0.3	1.8598
				0.4	2.0150

5 Summary of analysis

The analysis addresses the impact of the activation energy on squeezing flow Jeffery nano-liquids with bioconvection over two parallel disks. The boundary layer equation has been translated to nonlinear differential equations using the necessary dimensionless variables. Numerical effects are calculated using the built-in MATLAB tools bvp4c shooting scheme. The primary contact pints are seen below:

- An increment in squeezing parameter and mixed convection parameter lead flow of fluid.
- The temperature diminishes for greater variation of Prandtl number.
- The temperature field improves for larger Brownian motion parameter and thermophoresis parameter.
- The concentration of nanoparticles profile is a diminishing role of thermophoresis parameter and activation energy.
- The microorganisms filed reduce significantly with booming the estimation of Peclet number and bio-convection Lewis number.

Author contributions: All the authors have accepted responsibility for the entire content of this submitted manuscript and approved submission.

Research funding: The research was supported by the National Natural Science Foundation of China (Grant Nos. 11971142, 11871202, 61673169, 11701176, 11626101, 11601485).

Conflict of interest statement: The authors declare no conflicts of interest regarding this article.

References

Atif, S. M., S. Hussain, and M. Sagheer. 2019. "The Magnetohydrodynamic Stratified Bioconvective Flow of Micropolar Nanofluid Due to Gyrotactic Microorganisms." *AIP Advances* 9 (2): 025208.

Aleem, M., M. I. Asjad, A. Ahmadian, M. Salimi, and M. Ferrara. 2020. "Heat Transfer Analysis of Channel Flow of MHD Jeffrey Fluid Subject to Generalized Boundary Conditions." *The European Physical Journal Plus* 135 (1): 1–15.

Anwar, T., P. Kumam, and W. Watthayu. 2020. "An Exact Analysis of Unsteady MHD Free Convection Flow of Some Nanofluids with Ramped Wall Velocity and Ramped Wall Temperature Accounting Heat Radiation and Injection/consumption." *Scientific Reports* 10 (1): 1–19.

Alshomrani, A. S., and M. Ramzan. 2019. "Upshot of Magnetic Dipole on the Flow of Nanofluid along a Stretched Cylinder with Gyrotactic Microorganism in a Stratified Medium." *Physica Scripta* 95 (2): 025702.

Alwatban, A. M., S. U. Khan, H. Waqas, and I. Tlili. 2019. “Interaction of Wu’s Slip Features in Bioconvection of Eyring Powell Nanoparticles with Activation Energy.” *Processes* 7 (11): 859.

Buongiorno, J. 2006. “Convective Transport in Nanofluids.” *Journal of Heat Transfer* 128 (3): 240–50.

Babu, D. D., S. Venkateswarlu, and E. Keshava Reddy. 2019. “Multivariate Jeffrey Fluid Flow Past a Vertical Plate through Porous Medium.” *Journal of Applied and Computational Mechanics* 6 (3): 605–16.

Bozorg, M. V., M. H. Doranehgard, K. Hong, and Q. Xiong. 2020. “CFD Study of Heat Transfer and Fluid Flow in a Parabolic Trough Solar Receiver with Internal Annular Porous Structure and Synthetic Oil–Al_2O_3 Nanofluid.” *Renewable Energy* 145: 2598–614.

Choi, S. U. S. 1995. “Enhancing Thermal Conductivity of Fluids with Nanoparticles.” In *International Mechanical Engineering Congress and Exhibition, FED 231/MD*, 99–105, vol. 66.

Ghasemi, K. and M. Siavashi. 2020. “Three-dimensional Analysis of Magnetohydrodynamic Transverse Mixed Convection of Nanofluid inside a Lid-Drivenclosure Using MRT-LBM.” *International Journal of Mechanical Sciences* 165: 105199.

Hosseinzadeh, K., S. Salehi, M. R. Mardani, F. Y. Mahmoudi, M. Waqas, and D. D. Ganji. 2020. “Investigation of Nano-Bioconvective Fluid Motile Microorganism and Nanoparticle Flow by Considering MHD and Thermal Radiation.” *Informatics in Medicine Unlocked* 21: 100462.

Imran, N., M. Javed, M. Sohail, S. Farooq, and M. Qayyum. 2020. “Outcome of Slip Features on the Peristaltic Flow of a Rabinowitsch Nanofluid in an Asymmetric Flexible Channel.” *Multidiscipline Modeling in Materials and Structures*. https://doi.org/10.1108/MMMS-02-2020-0039.

Katta, R., and P. Jayavel. 2020. “Heat Transfer Enhancement in Radiative Peristaltic Propulsion of Nanofluid in the Presence of Induced Magnetic Field.” *Numerical Heat Transfer Part A: Applications*. https://doi.org/10.1080/10407782.2020.1835089.

Khan, M. I., M. Waqas, T. Hayat, and A. Alsaedi. 2017. “A Comparative Study of Casson Fluid with Homogeneous-Heterogeneous Reactions.” *Journal of Colloid and Interface Science* 498: 85–90.

Khan, M. I., M. U. Hafeez, T. Hayat, M. I. Khan, and A. Alsaedi. 2020. “Magneto Rotating Flow of Hybrid Nanofluid with Entropy Generation.” *Computer Methods and Programs in Biomedicine* 183: 105093.

Kuznetsov, A. V. 2011. “Nanofluid Bioconvection in Water-Based Suspensions Containing Nanoparticles and Oxytactic Microorganisms: Oscillatory Instability.” *Nanoscale Research Letters* 6 (1): 100.

Khan, S. U., A. Rauf, S. A. Shehzad, Z. Abbas, and T. Javed. 2019. “Study of Bioconvection Flow in Oldroyd-B Nanofluid with Motile Organisms and Effective Prandtl Approach.” *Physica A: Statistical Mechanics and its Applications* 527: 121179.

Khan, M. I., and F. Alzahrani. 2021. “Nonlinear Dissipative Slip Flow of Jeffrey Nanomaterial towards a Curved Surface with Entropy Generation and Activation Energy.” *Mathematics and Computers in Simulation* 185: 47–61.

Khan, M. I., S. U. Khan, M. Jameel, Y. M. Chu, I. Tlili, and S. Kadry. 2021. “Significance of Temperature-dependent Viscosity and Thermal Conductivity of Walter’s B Nanoliquid when Sinusodal Wall and Motile Microorganisms Density are Significant.” *Surfaces and Interfaces* 22: 100849.

Khan, M. I., and F. Alzahrani. 2021. “Free Convection and Radiation Effects in Nanofluid (Silicon Dioxide and Molybdenum Disulfide) with Second Order Velocity Slip, Entropy Generation, Darcy–Forchheimer Porous Medium.” *International Journal of Hydrogenergy* 46: 1362–9.

Li, F., M. Sheikholeslami, R. N. Dara, M. Jafaryar, A. Shafee, T. Nguyen-Thoi, and Z. Li. 2020. “Numerical Study for Nanofluid Behavior inside a Storage Finned Enclosure Involving Melting Process.” *Journal of Molecular Liquids* 297: 111939.

Nazeer, M., F. Hussain, M. O. Ahmad, S. Saeed, M. I. Khan, S. Kadry, and Y. M. Chu. 2021. “Multi-phase Flow of Jeffrey Fluid Bounded within Magnetized Horizontal Surface.” *Surfaces and Interfaces* 22: 100846.

Ramzan, M., H. Gul, J. D. Chung, S. Kadry, and Y. M. Chu. 2020. “Significance of Hall Effect and Ion Slip in a Three-Dimensional Bioconvective Tangent Hyperbolic Nanofluid Flow Subject to Arrhenius Activation Energy.” *Scientific Reports* 10: 1–15.

Ramzan, M., A. Rafiq, J. D. Chung, S. Kadry, and Y. M. Chu. 2020. “Nanofluid Flow with Autocatalytic Chemical Reaction over a Curved Surface with Nonlinear Thermal Radiation and Slip Condition.” *Scientific Reports* 10 (1): 1–13.

Rasool, G., A. Shafiq, and I. Tlili. 2020. “Marangoni Convective Nanofluid Flow over an Electromagnetic Actuator in the Presence of First-order Chemical Reaction.” *Heat Transfer – Asian Research* 49 (1): 274–88.

Sajjad, R. S., T. Muhammad, H. Sadia, and R. Ellahi. 2020. “The Hydromagnetic Flow of Jeffrey Nanofluid Due to a Curved Stretching Surface.” *Physica A: Statistical Mechanics and its Applications* 551: 124060.

Saffarian, M. R., M. Moravej, and M. H. Doranehgard. 2020. “Heat Transfer Enhancement in a Flat Plate Solar Collector with Different Flow Path Shapes Using Nanofluid.” *Renewable Energy* 146: 2316–29.

Turkyilmazoglu, M. 2020. “Single Phase Nanofluids in Fluid Mechanics and their Hydrodynamic Linear Stability Analysis.” *Computer Methods and Programs in Biomedicine* 187: 105171.

Tlili, I., H. Waqas, A. Almaneea, S. U. Khan, and M. Imran. 2019. “Activation Energy and Second-Order Slip in Bioconvection of Oldroyd-B Nanofluid over a Stretching Cylinder: A Proposed Mathematical Model.” *Processes* 7 (12): 914.

Waqas, H., S. U. Khan, M. Imran, and M. M. Bhatti. 2019. “Thermally Developed Falkner–Skan Bioconvection Flow of a Magnetized Nanofluid in the Presence of a Motile Gyrotactic Microorganism: Buongiorno’s Nanofluid Model.” *Physica Scripta* 94 (11): 115304.

Waqas, H., S. A. Shehzad, S. U. Khan, and M. Imran. 2019. “Novel Numerical Computations on Flow of Nanoparticles in Porous Rotating Disk with Multiple Slip Effects and Microorganisms.” *Journal of Nanofluids* 8 (7): 1423–32.

Yang, L., K. Du, and Z. Zhang. 2020. “Heat Transfer and Flow Optimization of a Novel Sinusoidal Minitube Filled with Non-Newtonian SiC/EG-Water Nanofluids.” *International Journal of Mechanical Sciences* 168: 105310.